PAPER • OPEN ACCESS

Interference effect on Goos–Hänchen shifts of anisotropic medium interface

To cite this article: Zihan Li *et al* 2023 *New J. Phys.* **25** 123018

IOP Publishing New J. Phys. 25 (2023) 123018 https://doi.org/10.1088/1367-2630/ad10ea

New Journal of Physics
The open access journal at the forefront of physics

Deutsche Physikalische Gesellschaft DPG
IOP Institute of Physics

Published in partnership with: Deutsche Physikalische Gesellschaft and the Institute of Physics

OPEN ACCESS

RECEIVED
30 May 2023

REVISED
2 October 2023

ACCEPTED FOR PUBLICATION
29 November 2023

PUBLISHED
8 December 2023

PAPER

Interference effect on Goos–Hänchen shifts of anisotropic medium interface

Zihan Li[1], **Ze Chen**[1,*], **Yong Li**[2,*], **Zhihai Zhang**[1], **Guoce Zhuang**[1], **Jianli Liu**[1] and **Yang Meng**[3]

[1] School of Physics and Electronic Engineering, Yancheng Teachers University, Yancheng, People's Republic of China
[2] School of Mechanical Engineering, University of Science and Technology Beijing, Beijing, People's Republic of China
[3] Institute of Mechanics, Chinese Academy of Sciences, Beijing, People's Republic of China
[*] Authors to whom any correspondence should be addressed.

E-mail: chenz@yctu.edu.cn and liyong@ustb.edu.cn

Keywords: Goos–Hänchen shift, spin-dependent interference, anisotropic medium

Abstract

We present a comprehensive analysis of the anomalous Goos–Hänchen (GH) displacement that occurs during the reflection of light beams at an interface between air and an anisotropic medium. This analysis also applies to the Imbert–Fedorov effect. Our study suggests that the anomalous GH displacement is primarily caused by polarization-dependent abnormal interference effects between the direct and cross-reflected light fields. Using the interface between air and a type II Weyl semimetal as an example, we provide a clear physical explanation for the relationship between spin-dependent abnormal interference effects and anomalous GH displacement. We demonstrate that spin-dependent constructive interference leads to a reduction in the GH displacement of the total reflected light field, while spin-dependent destructive interference results in an increase in the GH displacement of the total reflected light field.

1. Introduction

In the 17th century, Newton speculated that the center of a reflected light beam would experience a small spatial displacement, known as the Goos–Hänchen (GH) displacement, relative to its geometrically predicted position in the plane of incidence [1]. The quantitative measurement of GH displacement under total internal reflection was achieved by Goos and Hänchen in 1947 [2]. Subsequently, Artman, in 1948, attributed the GH displacement to the dispersion of reflection or transmission coefficients [3]. Typically, the GH displacement occurs at subwavelength scales [4]. In recent years, its importance has grown due to its sensitivity to changes in optical interface parameters [5–8]. It affects the modes of optical waveguides and microcavities [9–13], and offers potential for the design of new optical sensors [14, 15]. Consequently, understanding the mechanisms underlying GH displacement generation [16–28] and developing techniques for manipulating GH displacement [29–36] have become significant research pursuits. Some representative work on GH shift is as follows: (1) Li has proposed a unified theory describing the GH and the Imbert–Fedorov (IF) displacement by representing the vector angular spectrum of the three-dimensional beam in terms of two forms of angular spectrum composed of two orthogonal polarization components [17]. Using this unified theory, it can be clearly revealed that the eigenstates of GH displacement are two orthogonal linear polarizations, and the eigenstates of IF displacement are two orthogonal circular polarizations. (2) Aiello has proposed a method based on the functional shape of the light beams and functional shifts to unambiguously separate GH and IF shifts determined by beam shape distribution. It is proved that this separation is possible due to some general characteristics of the displacement distribution function for structured light beams [22]. Using this theory, the analytical expressions of the GH displacement and IF displacement (both spatial and angular) reflected by the vortex beam through the air-isotropic medium interface are perfectly derived. (3) Zhen *et al* have perfectly solved the mathematical description of GH displacement for Airy light beams on graphene and it showed that the GH shift can be modulated by the incident angle, the incident wavelength, the Fermi energy of graphene, the decay factors of Airy beams[32].

More recently, there has been increasing interest in studying GH displacement at anisotropic interfaces, including chiral metamaterials [37, 38], graphene-on-substrate systems [39–41], and semimetal metamaterials [42–44]. Previous studies have extensively examined the variations of anisotropic interface parameters on GH displacement and explored methods for manipulating it. In particular, the GH displacement at the interface of anisotropic materials can exhibit a series of abnormal phenomena due to the existence of cross Fresnel coefficient. However, the understanding of the physical mechanism behind the abnormal GH displacement has been stagnant. It is already known that interference effects play a crucial role in the generation of the GH displacement. In the case of an anisotropic interface, both directly reflected light field and cross-reflected light field contribute to the total reflected light field. The interference between these two reflected light fields leads to various intriguing optical phenomena associated with the GH displacement. However, the influence of the interference between the direct and cross-reflected light fields on the anomalous changes in GH displacement, as well as the quantification of the interference strength, have received limited attention in the literature.

The structure of this study is as follows. Firstly, we provide a comprehensive description of the GH displacement that occurs when arbitrarily polarized beams are reflected at the interface between air and an anisotropic medium. Subsequently, we elucidate the physical significance of the interference term between the direct reflected light field and the cross-reflected light field, introducing the concept of polarization-dependent abnormal interference effect in GH displacement. Moreover, we introduce a novel physical quantity, the abnormal interference factor, which quantifies the intensity of the interference effect. Taking type II Weyl semi-metal (WSM) as an example, a series of anomalies of GH displacement at the anisotropic interface are explained by analyzing the abnormal interference effect of spin correlation. Our findings demonstrate that the spin-dependent abnormal interference effect can serve as a characterization tool for determining the degree of tilt of the Weyl nodes in type II WSMs. Furthermore, we present a clear examination of the spin effect on the interference intensity between the direct reflected light field and the cross-reflected light field, as well as the self-intensity of each reflected light field. The superposition of these effects gives rise to anomalous GH displacement.

2. Theory and model

The plane of incidence is located in the x–z plane of the laboratory coordinate system (x, y, z). The unit vectors $\hat{\mathbf{x}}^a$, $\hat{\mathbf{y}}^a$ and $\hat{\mathbf{z}}^a$ represent the basis of the Cartesian coordinate system for the ath beam, where the superscript $a = i$ and r represent the incident and reflected beams respectively. The angular spectrum of the electric field for the polarized beam may be written as follows:

$$\left|\tilde{\boldsymbol{E}}^i\left(k_x^i, k_y^i\right)\right\rangle = C\left(a_P\left|P^i\right\rangle + a_S\left|S^i\right\rangle\right)\tilde{u}^i\left(k_x^i, k_y^i\right), \tag{1}$$

where complex amplitudes $a_P = \cos\alpha$ and $a_S = \sin\alpha\exp(i\Delta\phi)$ are the Jones representation of the state of polarization of the incident beam, and complex scalar function $\tilde{u}^i(k_x^i, k_y^i) = \exp[-\frac{(k_x^i)^2+(k_y^i)^2}{4}w_0^2]$ determines the distribution of the incident beam in Fourier space. The phase difference between the P and S components is given by $\Delta\phi$, while α and w_0 denote the amplitude ratio angle [45] and beam waist size of the incident beam, respectively. $\left|P^i\right\rangle = (1,0)^\dagger$ and $\left|S^i\right\rangle = (0,1)^\dagger$ represent the matrix description of the incident beam base vector along $\hat{x}^r$ and $\hat{y}^r$ directions respectively, where † represents the transposed conjugate of the matrix. Equation (1) is essentially the angular spectrum form of an arbitrarily polarized incident beam, and can also be understood as a mathematical description of an arbitrarily polarized beam in momentum space.

Thus, the angular spectrum representation of the transverse electric field of the reflected beam can be obtained:

$$\left|\tilde{\boldsymbol{E}}^r\right\rangle = \hat{M}_{l\to o}^r\hat{S}^r\hat{F}^r\hat{M}_{o\to l}^i\left(a_P\left|P^i\right\rangle + a_S\left|S^i\right\rangle\right)\tilde{u}^i\left(k_x^i, k_y^i\right) \tag{2}$$

with $\hat{M}_{o\to l}^i = \begin{pmatrix} 1 & \frac{k_y^i}{k}\cot\theta_i \\ -\frac{k_y^i}{k}\cot\theta_i & 1 \end{pmatrix}$; $\hat{M}_{l\to o}^r = \begin{pmatrix} 1 & -\frac{k_y^r}{k^r}\cot\theta_r \\ \frac{k_y^r}{k^r}\cot\theta_r & 1 \end{pmatrix}$;

$$\hat{F}^r = \begin{pmatrix} r_{PP}(1+\frac{1}{r_{PP}}\frac{\partial r_{PP}}{\partial\theta_i}\frac{k_x^i}{k^i}) & r_{PS}(1+\frac{1}{r_{PS}}\frac{\partial r_{PS}}{\partial\theta_i}\frac{k_x^i}{k^i}) \\ r_{SP}(1+\frac{1}{r_{SP}}\frac{\partial r_{SP}}{\partial\theta_i}\frac{k_x^i}{k^i}) & r_{SP}(1+\frac{1}{r_{SP}}\frac{\partial r_{SP}}{\partial\theta_i}\frac{k_x^i}{k^i}) \end{pmatrix}$$

where $\hat{M}_{l\to o}^r$ and $\hat{M}_{l\to o}^r$ are the transformation matrix from the incident central coordinate system to the incident local coordinate system and the transformation matrix from the reflected local coordinate system to the reflected central coordinate system respectively. The derivation of the $\hat{M}_{l\to o}^r$ and $\hat{M}_{l\to o}^r$ expressions has

been given in detail in the pioneering work of Bliokh, Li and Aiello *et al* on GH displacement [4, 17, 46, 47]. $\hat{F}^r$ is the Fresnel coefficient matrix. It is worth noting that the matrix element of $\hat{F}^r$ can be regarded as a Taylor expansion in the form of the angular spectrum of Fresnel coefficients, and it is clear that this matrix is sufficiently accurate under paraxial conditions. $\hat{S}^r$ is the scattering operator with mirror symmetry, which satisfies the following operation rules: $\hat{S}^r|\tilde{E}^r(k_x^i,k_y^i)\rangle = |\tilde{E}^r(k_x^i \mapsto -k_x^r, k_y^i \mapsto k_y^r)\rangle$. Using the inverse Fourier transform of equation (2), the electric field of the reflected beam in coordinate space can be written as:

$$|\boldsymbol{E}^r\rangle = \sum\nolimits_{j=P}^{S}\sum_{i=P}^{S}\int_{-\infty}^{+\infty}\int_{-\infty}^{+\infty} r_{ij}a_j\tilde{u}_L^r \exp\left(i\varphi_{ij}^r\right) dk_x^r dk_y^r |i^r\rangle, i \in \{P,S\}; j \in \{P,S\}. \tag{3}$$

with $\varphi_{ij}^r = k_x^r(x^r - \tilde{x}_{ij}^r) + k_y^r(y^r - \tilde{y}_{ij}^r) + k^r[1 - \frac{(k_x^r)^2+(k_y^r)^2}{2(k^r)^2}]z^r$,

$$\tilde{x}_{ij}^r = -i\frac{1}{2k}\frac{\partial\left[\ln\left(r_{ij}\right)^2\right]}{\partial\theta_i}, j = PP, PS, SP, SS$$

$$\tilde{y}_{ij=PP\mapsto SS}^r = \pm i\frac{a_{S\mapsto P}}{a_{P\mapsto S}}\frac{1}{k}\left(1 + \frac{r_{ij=SS\mapsto PP}}{r_{ij=PP\mapsto SS}}\right)\cot\theta_i, \tilde{y}_{ij=PP}^r \text{ take`} + \text{'}, \tilde{y}_{ij=SS}^r \text{ take`} - \text{'};$$

$$\tilde{y}_{ij=PS\mapsto SP}^r = \mp i\frac{a_{P\mapsto S}}{a_{S\mapsto P}}\frac{1}{k}\left(1 - \frac{r_{ij=SP\mapsto PS}}{r_{ij=PS\mapsto SP}}\right)\cot\theta_i, \tilde{y}_{ij=PS}^r \text{ take`} - \text{'}, \tilde{y}_{ij=SP}^r \text{ take '} + \text{'}.$$

The result after the integral operation of equation (3) is:

$$|\boldsymbol{E}^r\rangle = \left|\boldsymbol{E}_{P(\mathrm{D})}^r\right\rangle + \left|\boldsymbol{E}_{P(\mathrm{C})}^r\right\rangle + \left|\boldsymbol{E}_{S(\mathrm{D})}^r\right\rangle + \left|\boldsymbol{E}_{S(\mathrm{C})}^r\right\rangle, \tag{4}$$

with

$$\left|\boldsymbol{E}_{P(\mathrm{D})}^r\right\rangle = r_{PP}a_P u^r\left(x^r - \tilde{x}_{PP}^r, y^r - \tilde{y}_{PP}^r, z^r\right)|P^r\rangle, \left|\boldsymbol{E}_{P(\mathrm{C})}^r\right\rangle = r_{PS}a_S u^r\left(x^r - \tilde{x}_{PS}^r, y^r - \tilde{y}_{PS}^r, z^r\right)|P^r\rangle,$$

$$\left|\boldsymbol{E}_{S(\mathrm{D})}^r\right\rangle = r_{SP}a_P u^r\left(x^r - \tilde{x}_{SP}^r, y^r - \tilde{y}_{SP}^r, z^r\right)|S^r\rangle, \left|\boldsymbol{E}_{S(\mathrm{C})}^r\right\rangle = r_{SS}a_S u^r\left(x^r - \tilde{x}_{SS}^r, y^r - \tilde{y}_{SS}^r, z^r\right)|S^r\rangle$$

where $|\boldsymbol{E}_{P(\mathrm{D})}^r\rangle$ and $|\boldsymbol{E}_{S(\mathrm{D})}^r\rangle$ respectively represent reflected light fields caused by isotropic Fresnel coefficients in the directions P and S, while $|\boldsymbol{E}_{P(\mathrm{C})}^r\rangle$ and $|\boldsymbol{E}_{S(\mathrm{C})}^r\rangle$ respectively represent reflected light fields caused by anisotropic Fresnel coefficients in the directions P and S. The second and fourth terms in the right side of equation (4) are due to the non-zero anti-diagonal matrix element of Fresnel's equation, which is the fundamental reason why the GH displacement of the interface of anisotropic medium is different from that of the interface of isotropic medium. $u^r(x^r - \tilde{x}_{ij}^r, y^r - y_{ij}^r, z^r)$ can be understood as a function shift. The centroid of the reflected beam can be expressed as:

$$\Delta_{\mathrm{GH}}^r = \frac{\langle\boldsymbol{E}^r|\,x^r\,|\boldsymbol{E}^r\rangle}{\langle\boldsymbol{E}^r|\,\boldsymbol{E}^r\rangle}. \tag{5}$$

By combining equations (4) and (5), it is not difficult to obtain detailed expressions that can reveal the influence of the interference effect of the $|\boldsymbol{E}_{P/S(\mathrm{D})}^r\rangle$ and $|\boldsymbol{E}_{P/S(\mathrm{C})}^r\rangle$ light fields, and the self-intensity of the $|\boldsymbol{E}_{P/S(\mathrm{D})}^r\rangle$ and $|\boldsymbol{E}_{P/S(\mathrm{C})}^r\rangle$ light fields on GH displacement

$$\Delta_{\mathrm{GH}}^r = \Delta_{\mathrm{GH-D}}^r + \Delta_{\mathrm{GH-C}}^r + \Delta_{\mathrm{GH-DC}}^r, \tag{6}$$

with

$$\Delta_{\mathrm{GH-D}}^r = \frac{\sum_{j=P}^{S}\left\langle\boldsymbol{E}_{j(\mathrm{D})}^r\middle|\,x^r\,\middle|\boldsymbol{E}_{j(\mathrm{D})}^r\right\rangle}{\sum_{j=P}^{S}\left\langle\boldsymbol{E}_{j(\mathrm{D})}^r\middle|\,\boldsymbol{E}_{j(\mathrm{D})}^r\right\rangle + 2\mathrm{Re}\left[\sum_{j=P}^{S}\left\langle\boldsymbol{E}_{j(\mathrm{D})}^r\middle|\,\boldsymbol{E}_{j(\mathrm{C})}^r\right\rangle\right] + \sum_{j=P}^{S}\left\langle\boldsymbol{E}_{j(\mathrm{C})}^r\middle|\,\boldsymbol{E}_{j(\mathrm{C})}^r\right\rangle}$$

$$\Delta_{\mathrm{GH-C}}^r = \frac{\sum_{j=P}^{S}\left\langle\boldsymbol{E}_{j(\mathrm{C})}^r\middle|\,x^r\,\middle|\boldsymbol{E}_{j(\mathrm{C})}^r\right\rangle}{\sum_{j=P}^{S}\left\langle\boldsymbol{E}_{j(\mathrm{D})}^r\middle|\,\boldsymbol{E}_{j(\mathrm{D})}^r\right\rangle + 2\mathrm{Re}\left[\sum_{j=P}^{S}\left\langle\boldsymbol{E}_{j(\mathrm{D})}^r\middle|\,\boldsymbol{E}_{j(\mathrm{C})}^r\right\rangle\right] + \sum_{j=P}^{S}\left\langle\boldsymbol{E}_{j(\mathrm{C})}^r\middle|\,\boldsymbol{E}_{j(\mathrm{C})}^r\right\rangle},$$

$$\Delta_{\mathrm{GH-DC}}^r = \frac{\sum_{j=P}^{S}\left\langle\boldsymbol{E}_{j(\mathrm{D})}^r\middle|\,x^r\,\middle|\boldsymbol{E}_{j(\mathrm{C})}^r\right\rangle]}{\sum_{j=P}^{S}\left\langle\boldsymbol{E}_{j(\mathrm{D})}^r\middle|\,\boldsymbol{E}_{j(\mathrm{D})}^r\right\rangle + 2\mathrm{Re}[\sum_{j=P}^{S}\left\langle\boldsymbol{E}_{j(D)}^r\middle|\,\boldsymbol{E}_{j(\mathrm{C})}^r\right\rangle] + \sum_{j=P}^{S}\left\langle\boldsymbol{E}_{j(\mathrm{C})}^r\middle|\,\boldsymbol{E}_{j(\mathrm{C})}^r\right\rangle}.$$

Here, terms $\sum_{j=P}^{S}\langle \boldsymbol{E}_{j(\mathrm{D})}^{r}|\boldsymbol{E}_{j(\mathrm{D})}^{r}\rangle$ and $\sum_{j=P}^{S}\langle \boldsymbol{E}_{j(\mathrm{C})}^{r}|\boldsymbol{E}_{j(\mathrm{C})}^{r}\rangle$ represent the self-intensity of the direct reflected light field and cross-reflected light field respectively, while terms $2\mathrm{Re}[\sum_{j=P}^{S}\langle \boldsymbol{E}_{j(\mathrm{D})}^{r}|\boldsymbol{E}_{j(\mathrm{C})}^{r}\rangle]$ represent the interference between the direct reflected light field and cross-reflected light field, and the intensity of the interference is related to the spin of the incident light, which is called anomalous interference. It is worth noting that the abnormal interference term itself also generates abnormal GH displacement, which is reflected in the $\sum_{j=P}^{S}\langle \boldsymbol{E}_{j(D)}^{r}|x^{r}|\boldsymbol{E}_{j(C)}^{r}\rangle]$ terms in the molecule of equation (6). The influence of the abnormal interference effect between the direct reflected light field and cross-reflected light field on the generating mechanism of the abnormal GH displacement is the focus of this work. After a simple derivation, terms $\Delta_{\mathrm{GH-D}}^{r}$, $\Delta_{\mathrm{GH-C}}^{r}$, and $\Delta_{\mathrm{GH-DC}}^{r}$ in equation (6) can be written respectively

$$\Delta_{\mathrm{GH-D}}^{r} = -\frac{\mathrm{Im}\left(\tilde{x}_{\mathrm{D}}^{r}\right)}{N_0\left(1+N_{x/s}\right)}, \tag{7}$$

$$\Delta_{\mathrm{GH,C}}^{r} = -\frac{\mathrm{Im}\left(\tilde{x}_{\mathrm{C}}^{r}\right)}{N_0\left(1+N_{x/s}\right)}, \tag{8}$$

$$\Delta_{\mathrm{GH-DC}}^{r} = -\frac{\mathrm{Im}\left(\tilde{x}_{\mathrm{DC}}^{r}\right)}{N_0\left(1+N_{x/s}\right)}, \tag{9}$$

with

$$\tilde{x}_{\mathrm{D}}^{r} = -\frac{1}{2k}\left(|r_{PP}a_P|^2\frac{\partial r_{PP}}{r_{PP}\partial\theta_i}+|r_{SS}a_S|^2\frac{\partial r_{SS}}{r_{SS}\partial\theta_i}\right)\quad \tilde{x}_{\mathrm{C}}^{r} = -\frac{1}{2k}\left\{|r_{PS}a_S|^2\frac{\partial r_{PS}}{\partial r_{PS}\partial\theta_i}+|r_{SP}a_P|^2\frac{\partial r_{SP}}{r_{SP}\partial\theta_i}\right\}$$

$$\tilde{x}_{\mathrm{DC}}^{r} = -\frac{1}{4k}\left[\rho\left(r_{PS}{}^{*}\frac{\partial r_{PP}}{\partial\theta_i}+r_{SP}{}^{*}\frac{\partial r_{SS}}{\partial\theta_i}+r_{PP}{}^{*}\frac{\partial r_{PS}}{\partial\theta_i}+r_{SS}{}^{*}\frac{\partial r_{SP}}{\partial\theta_i}\right)\right.$$

$$\left.+i\sigma\left(r_{PP}{}^{*}\frac{\partial r_{PS}}{\partial\theta_i}+r_{SS}{}^{*}\frac{\partial r_{SP}}{\partial\theta_i}-r_{PS}{}^{*}\frac{\partial r_{PP}}{\partial\theta_i}-r_{SP}{}^{*}\frac{\partial r_{SS}}{\partial\theta_i}\right)\right]\quad N_0 = |r_{PP}a_P|^2+|r_{PS}a_S|^2+|r_{SP}a_P|^2+|r_{SS}a_S|^2$$

$$N_{x/s} = [\rho\mathrm{Re}(r_{PP}r_{PS}{}^{*}+r_{SP}r_{SS}{}^{*})+\sigma\mathrm{Im}(r_{PP}r_{PS}{}^{*}+r_{SP}r_{SS}{}^{*})]/(|r_{PP}a_P|^2+|r_{PS}a_S|^2+|r_{SP}a_P|^2+|r_{SS}a_S|^2),$$

where σ=2Im$(a_P^{*}a_S)$ is the degree of spin of the incident light beams; ρ=2Re$(a_P^{*}a_S)$ is the degree of linear polarization inclined at 45° angle of the incident light beams [4]. Obviously, $\Delta_{\mathrm{GH-D}}^{r}$, $\Delta_{\mathrm{GH,C}}^{r}$, and $\Delta_{\mathrm{GH-DC}}^{r}$ are closely related to the polarization of the incident light field. It is worth noting that for weakly anisotropic media, equations (7)–(9) hold only when the incident beam waist radius is much larger than the total GH displacement. In addition, when an anisotropic medium is replaced by an isotropic medium, equations (8) and (9) are zero. Interestingly, since the eigenbasis of Fresnel's equation for polarized beams at the interface of anisotropic media is not linearly polarized basis, GH displacement exhibits a complex relationship related to polarization. Specifically, GH displacement is related to both polarization parameters ρ of linearly polarized light and σ of circularly polarized light. The abnormal GH displacement reflected at the anisotropic interface is mainly from the abnormal interference effect, which is reflected in the normalization factor $N_{x/s}$ of equations (7)–(9), as well as the molecular part of the equation (9). It is not difficult to find that this interference is closely related to the state of polarization of the incident light. It should be emphasized here that $N_{x/s}$ can essentially be regarded as a physical quantity that measures the strength of the polarization-dependent abnormal interference effect. So in this work, the deeper physical meaning of $N_{x/s}$ is thoroughly revealed. Since $N_{x/s}$ reflects the relative magnitude of abnormal interference intensity between direct reflected light field and cross-reflected light field compared with the total reflected light field intensity, it is called an abnormal interference factor. To the best of our knowledge, the concept of polarization-dependent abnormal interference is introduced to analyze the physical mechanism of the abnormal GH displacement at the anisotropic medium interface, which is proposed for the first time. The effect of spin-dependent abnormal interference on the abnormal GH displacement is the main conclusion of our work.

3. Numerical results and analysis

The topological Fermi arc on the type II WSM (MoTe2) was first experimentally observed in 2016, confirming the existence of the type II Weyl fermion that destroys Lorentz invariance in real materials [48]. The discovery of the type II WSM not only establishes the link between particle physics and condensed matter but also may lead to new applications in the field of optoelectronics [49, 50]. To find more novel

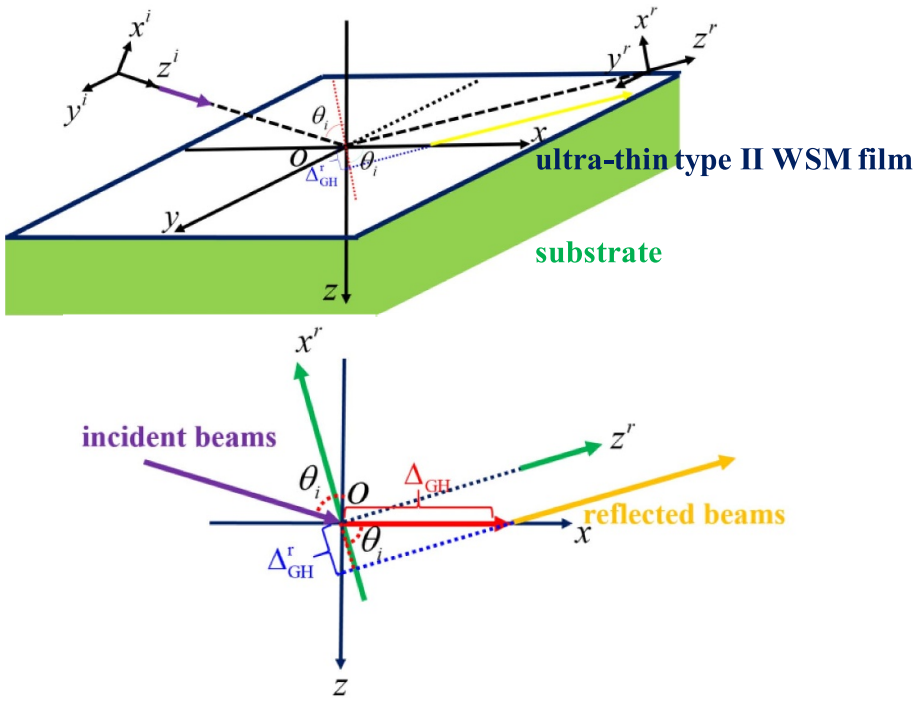

Figure 1. Structure diagram of the reflected light from the type II WSM film. Where $\Delta^{r}_{GH} = -\Delta_{GH}/\cos\theta_i$. θ_i is the incident angle.

anomalous effects in spin photonics, the combination between the Type II WSM and beam displacement has become the focus of attention in recent years [51–57]. In this section, we take the Type II WSM film as an example and focus on analyzing the influence of abnormal interference between the reflected light field and the cross-reflected light field on GH displacement for the anisotropic medium interface. The analytical expression of Fresnel's equation for polarized light oblique impinging at the air-WSM interface can be expressed as follows (see appendix A for detailed derivation):

$$r_{PP} = \frac{\left(n_2\cos\theta_i - n_1\cos\theta_t + Z_0\sigma^S_{xx}\cos\theta_i\cos\theta_t\right)\left(n_1\cos\theta_i + n_2\cos\theta_t + Z_0\sigma^S_{yy}\right) - Z_0^2\sigma^S_{xy}\sigma^S_{yx}\cos\theta_i\cos\theta_t}{\Delta}, \tag{10}$$

$$r_{SS} = \frac{\left(n_1\cos\theta_t + n_2\cos\theta_i + Z_0\sigma^S_{xx}\cos\theta_i\cos\theta_t\right)\left(n_1\cos\theta_i - n_2\cos\theta_t - Z_0\sigma^S_{yy}\right) + Z_0^2\sigma^S_{xy}\sigma^S_{yx}\cos\theta_i\cos\theta_t}{\Delta}, \tag{11}$$

$$r_{PS} = -r_{SP} = \frac{2n_1 Z_0\sigma^S_{xy}\cos\theta_i\cos\theta_t}{\Delta}, \tag{12}$$

with

$$\Delta = (n_2\cos\theta_i + n_1\cos\theta_t + Z_0\sigma^S_{xx}\cos\theta_i\cos\theta_t)(n_1\cos\theta_i + n_2\cos\theta_t + Z_0\sigma^S_{yy}) - Z_0^2\sigma^S_{xy}\sigma^S_{yx}\cos\theta_i\cos\theta_t,$$
$$\cos\theta_t = (1 - {n_1}^2\sin^2\theta_i/{n_2}^2)^{1/2}$$

where Z_0 is the wave impedance in vacuum, σ^S_{ij} $(ij = xx, xy, yx, yy)$ is the transverse optical conductivity, the refractive index of air, and the substrate material of type II WSM is n_1 and n_2 respectively. We assume that an arbitrarily polarized Gaussian beam impinges on the surface of an ultra-thin type II WSM film with no Fermi arc state at the incident angle θ_i, as shown in figure 1. The angular GH displacement is ignored in figure 1.

According to the analysis in the previous section, the abnormal interference phenomenon of direct reflected light field and cross-reflected light field can be reflected by the size of the abnormal interference factor $N_{x/s}$. In the following numerical simulation, the wavelength λ was selected as 632.8 nm (The expression of the type II WSM film transverse optical conductivity corresponding to the wavelength is given in appendix B). It can be seen from figures 2(a)–(c) that large abnormal interference factors $N_{x/s}$ occur in a small angular wide range of polarization angles α close to zero. In order to further determine the angular

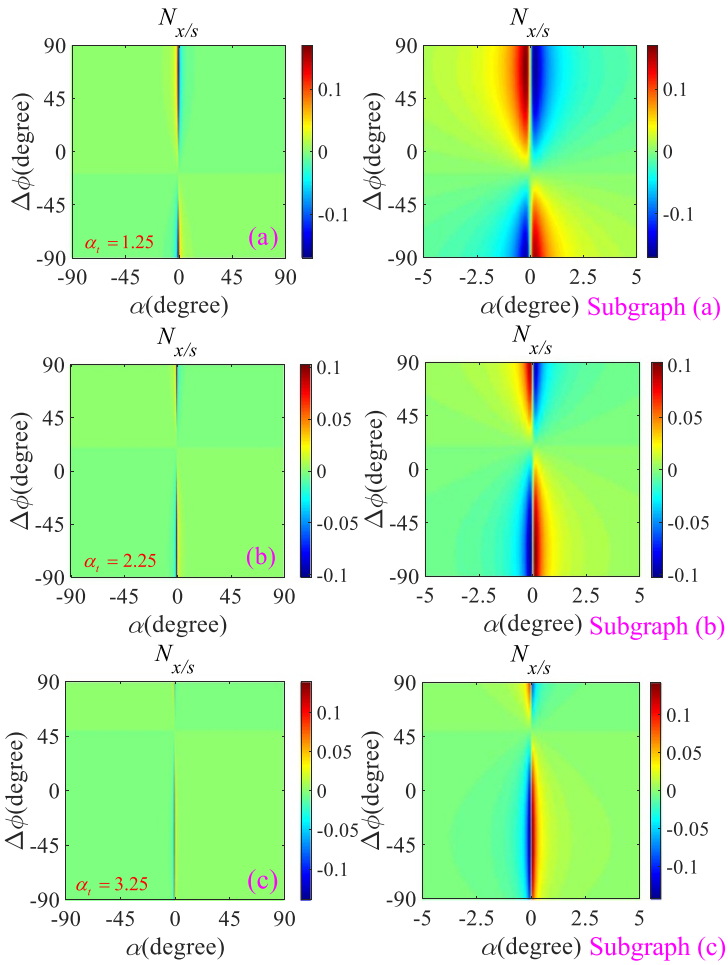

Figure 2. Two-dimensional image of the abnormal interference factor $N_{x/s}$ varying with the polarization state of incident light. (a) $\alpha_t = 1.25$; $\theta_i = \theta_i^{pB} = 75.8^o$ (b) $\alpha_t = 2.25$; $\theta_i = \theta_i^{pB} = 75.7^o$ (c) $\alpha_t = 3.25$; $\theta_i = \theta_i^{pB} = 75.6^o$.

width of the amplitude ratio angle α and the phase difference $\Delta\phi$, the size distribution of the interference factor is clearly shown at the amplitude ratio angle α from $-5°$ to $+5°$, and the phase difference $\Delta\phi$ from $-90°$ to $90°$, as shown in the subgraphs of figures 2(a)–(c). It is not difficult to find that large anomalous interference factors $N_{x/s}$ can appear in a wide range of phase differences $\Delta\phi$ and a narrow range of amplitude ratio angle α. This means that the abnormal interference effects are very sensitive to the change of amplitude ratio angle α and very insensitive to the change of phase difference $\Delta\phi$. Meanwhile, further analysis shows that the maximum value of the abnormal interference factor $N_{x/s}$ corresponding to the degree of tilt $\alpha_t = 1.25$ is significantly larger than that corresponding to the degree of tilt $\alpha_t = 2.25$. Although the interference factor for degree of tilt $\alpha_t = 1.25$ is not much different from that with the degree of tilt $\alpha_t = 3.25$, the larger interference factor for the $\alpha_t = 1.25$ occurs in a larger amplitude ratio angle range than that with the degree of tilt $\alpha_t = 3.25$. This means that the anomalous GH displacement phenomenon can be easily displayed when the degree of tilt α_t is equal to 1.25, and the incident angle is close to the pseudo-Brewster angle. It should be pointed out that the variation of abnormal interference factors $N_{x/s}$ with optical parameters and interface parameters is analyzed numerically to quantitatively control the strength of polarization-dependent abnormal interference effects. In other words, the abnormal interference factor $N_{x/s}$ is a mathematical description of the strength of polarization-dependent abnormal interference effects.

In order to further reveal the relationship between the abnormal interference factor $N_{x/s}$ near the pseudo-Brewster angle and the tilt degrees α_t of type II WSM film, figure 3 shows the physical picture of the abnormal interference factor $N_{x/s}$ changing with the tilt degrees α_t of the type II WSM film and the incident angle of the incident light when the polarization state of the incident light remains constant. It should be emphasized that different degrees of tilt α_t correspond to different pseudo-Brewster angles θ_i^{pB}. By comparing figure 3(a) with figures 3(d), (b) with figure 3(e), and figure 3(c) with figure 3(f), when the amplitude ratio angle is constant, the polarization-dependent abnormal interference effect corresponding to the phase difference $\Delta\phi$ of $90°$ is stronger than that corresponding to the phase difference $\Delta\phi$ of $0°$. It

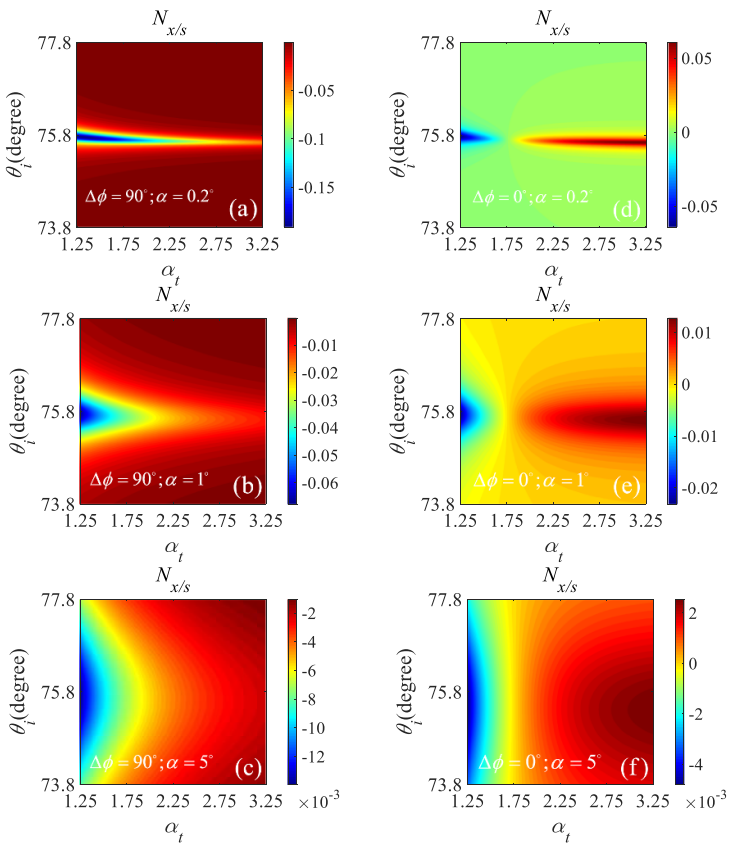

Figure 3. The abnormal interference factor $N_{x/s}$ versus the incident angle θ_i and the title degrees α_t of the type II WSM film. (a) $\Delta\phi = 90^o, \alpha = 0.2^o$; (b) $\Delta\phi = 90^o, \alpha = 1^o$; (c) $\Delta\phi = 90^o, \alpha = 5^o$;(*e*). (d) $\Delta\phi = 0^o, \alpha = 0.2^o$; (e) $\Delta\phi = 0^o, \alpha = 1^o$; (f) $\Delta\phi = 90^o, \alpha = 5^o$.

should be noted here that when the phase difference $\Delta\phi$ of the incident light is equal to 90°, then $\rho = 0$. $N_{x/s}$ can be regarded as a spin-dependent abnormal interference factor, which can be used to characterize the strength of the spin-dependent abnormal interference effect in reflected light. Figure 3(a) clearly shows that the spin-dependent abnormal interference effect becomes stronger at a tilt factor α_t of 1.25 and an amplitude ratio angle α of 0.2°, while figure 3(c) clearly shows that the spin-dependent abnormal interference effect almost disappears at a tilt factor α_t of 1.25 and an amplitude ratio angle α of 5°. In order to further explore the influence of spin-dependent abnormal interference effect on GH displacement, it is obviously necessary to select the polarization parameter of incident beam phase difference $\Delta\phi$ as 90°. Therefore, using the relationship between spin-dependent abnormal interference effect and tilt degrees α_t, it is expected to provide a new technical method to characterize the tilt degrees α_t of the type II WSM film. It also opens up a new way to characterize the physical parameters of an anisotropic medium by spin optical effect.

It can be seen from the theoretical derivation in the previous section that the relationship between GH displacement at the anisotropic interface and the polarization parameters of the incident beam is very complex, and the total GH displacement is determined by the three sub-GH displacements (including$\Delta^r_{\mathrm{GH-D}}$, $\Delta^r_{\mathrm{GH-C}}$ and $\Delta^r_{\mathrm{GH-DC}}$). Therefore, in order to thoroughly reveal the influence of spin-dependent abnormal interference effect on the total GH displacement, it is necessary to simulate the physical pictures of the $\Delta^r_{\mathrm{GH-D}}$, $\Delta^r_{\mathrm{GH-C}}$ and $\Delta^r_{\mathrm{GH-DC}}$ with the change of the amplitude ratio angle α. Next, from the perspective of the spin-dependent abnormal interference effect between direct reflected light field and cross-reflected light field, we focus on analyzing the physical mechanism of the abnormal phenomenon that the $\Delta^r_{\mathrm{GH-D}}$, $\Delta^r_{\mathrm{GH-C}}$ and $\Delta^r_{\mathrm{GH-DC}}$ change with the polarization state of incident light. According to equations (7)–(9), we can clearly show the trend of $\Delta^r_{\mathrm{GH-D}}$, $\Delta^r_{\mathrm{GH-C}}$ and $\Delta^r_{\mathrm{GH-DC}}$ changing with the amplitude ratio angle α of incident light for the $\theta_i = \theta_i^{pB} = 75.8^o$ and $\alpha_t = 1.25$, as shown in figure 4(a). Specifically, figure 4(a) shows that the $\Delta^r_{\mathrm{GH-D}}$ curve is no longer symmetric with the longitudinal axis, that is, the $\Delta^r_{\mathrm{GH-D}}$ corresponding to $\alpha = 0.1^\circ$ is obviously no longer equal to the $\Delta^r_{\mathrm{GH-D}}$ corresponding to $\alpha = -0.1^\circ$, which is obviously different from the characteristics of GH displacement reflected by the isotropic interface. From the previous analysis, it can be seen that this obvious difference is caused by the spin-dependent abnormal interference effect. A similar phenomenon can also be found in the variation trend

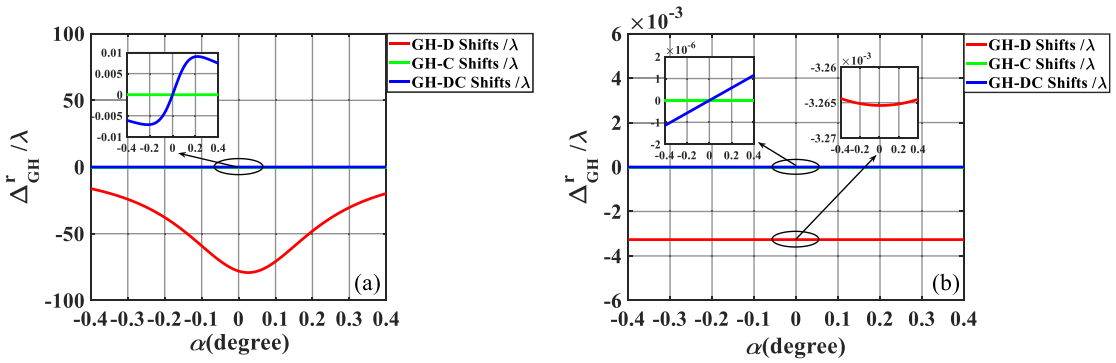

Figure 4. When the incident angle is equal to the pseudo-Brewster angle, the $\Delta^r_{\mathrm{GH-D}}$, $\Delta^r_{\mathrm{GH-C}}$ and $\Delta^r_{\mathrm{GH-DC}}$ change with the amplitude ratio angle α. (a) $\alpha_t = 1.25$, $\theta_i = \theta_i^{pB} = 75.8^o$, $\Delta\phi = 90^o$; (b) $\alpha_t = 1.25$, $\theta_i = 60^o$, $\Delta\phi = 90^o$.

of the $\Delta^r_{\mathrm{GH-C}}$ with the polarization state of incident light. Interestingly, the variation of $\Delta^r_{\mathrm{GH-DC}}$ with the state of polarization of incident light is very similar to the variation of IF displacement with isotropic interface reflection with the state of polarization of incident light, but the former is asymmetrical about the origin of coordinates (i.e., $\alpha = 0, \Delta\phi = 0$), while the latter is symmetric about the origin of coordinates. The abnormal phenomenon of $\Delta^r_{\mathrm{GH-DC}}$ is completely caused by the spin-dependent abnormal interference effect between the direct reflected light field and the cross-reflected light field, and the symmetry breaking can be quantified by the spin-dependent abnormal interference effect. Therefore, the anomalous phenomenon of GH displacement of polarized light at the Type II WSM film can also be manipulated by changing the spin-dependent abnormal interference effect. By further observing figure 4(a), and combining with the results of figure 3(a), it can be found that the abnormal effect of GH displacement decreases with the increase of the degree of tilt α_t of the Type II WSM. In other words, we can identify the magnitude of the degree of tilt α_t of the Type II WSM by calculating the strength of the abnormal interference factor$N_{x/s}$. It is worth noting that the abnormal GH displacement disappears when the incident angle is far away from the pseudo-Brewster angle, as shown in figure 4(b). This is because the *P* component of the direct reflected light field composed of the plane wavelets with slightly different wave vectors will change very slowly with the small change of the wave vector, which leads to the fact that the abnormal interference factor is almost zero. In short, the spin-dependent abnormal interference effect is the physical source of the abnormal phenomenon that the symmetry of the GH displacement curve is broken in different degrees.

To further demonstrate a clear physical picture, figure 5 shows the intensity distribution of the light field reflected by polarized light with the amplitude ratio angle $\alpha = -0.1°$ and $+0.1°$and the phase difference $\Delta\phi = 90°$ through the air-Type II WSM interface at $\theta_i = 75.8°$. It is easy to see the interference intensity between the $|\boldsymbol{E}^r_{j(\mathrm{D})}\rangle$ and $|\boldsymbol{E}^r_{j(\mathrm{C})}\rangle$, and the self-intensity of the $|\boldsymbol{E}^r_{j(\mathrm{D})}\rangle$ and $|\boldsymbol{E}^r_{j(\mathrm{C})}\rangle$ has Gaussian distribution. On the one hand, by observing figures 5(c) and (f), it can be further found that the abnormal interference intensity between the $|\boldsymbol{E}^r_{j(\mathrm{D})}\rangle$ and $|\boldsymbol{E}^r_{j(\mathrm{C})}\rangle$, corresponding to the incident spins of plus or minus 0.1 respectively, shows an obvious spin-dependent intensity distribution. On the other hand, the self-intensity distribution of the direct reflected light field shows a significant spin-independent GH shift, as shown in figures 5 (d) and (g), while the cross-reflected light field self-intensity distribution shows almost zero GH shift, as shown in figures 5(e) and (h). Interestingly, the superposition of the $|\boldsymbol{E}^r_{j(\mathrm{D})}\rangle$ and $|\boldsymbol{E}^r_{j(\mathrm{C})}\rangle$ results in a novel GH shift dependent on the spin of the incident light in the total light field intensity, i.e. $\Delta^r_{\mathrm{GH}}(\alpha = +0.1°, \Delta\phi = 90°) \neq \Delta^r_{\mathrm{GH}}(\alpha = -0.1°, \Delta\phi = 90°)$, as shown in figures 5(a) and (b). The above novel spin-dependent abnormal GH shifts are essentially caused by the coherent superpositions of the $|\boldsymbol{E}^r_{j(\mathrm{D})}\rangle$ and $|\boldsymbol{E}^r_{j(\mathrm{C})}\rangle$. It is worth emphasizing that the influence of coherent superposition of $|\boldsymbol{E}^r_{j(\mathrm{D})}\rangle$ and $|\boldsymbol{E}^r_{j(\mathrm{C})}\rangle$ on the calculation results of the $\Delta^r_{\mathrm{GH-D}}$, $\Delta^r_{\mathrm{GH-C}}$ and $\Delta^r_{\mathrm{GH-DC}}$ is due to the consideration of the total light field normalization factor. In other words, spin-dependent constructive interference leads to a decrease in GH of the total reflected light field, while spin-dependent destructive interference leads to an increase in GH displacement of the total reflected light field. So far, the physical mechanism of anomalous GH displacement is deeply revealed from the perspective of spin-dependent abnormal interference between $|\boldsymbol{E}^r_{j(\mathrm{D})}\rangle$ and $|\boldsymbol{E}^r_{j(\mathrm{C})}\rangle$ light fields (i.e. the interference appears one positive and one negative). More importantly, the intensity distribution of the light field simulated by equation (4) as shown in figure 5 is exactly the same as the GH displacement image simulated by equations (7)–(9) as shown in figure 4(a), which shows that equations (7)–(9) of the main theoretical derivation results can be indirectly verified.

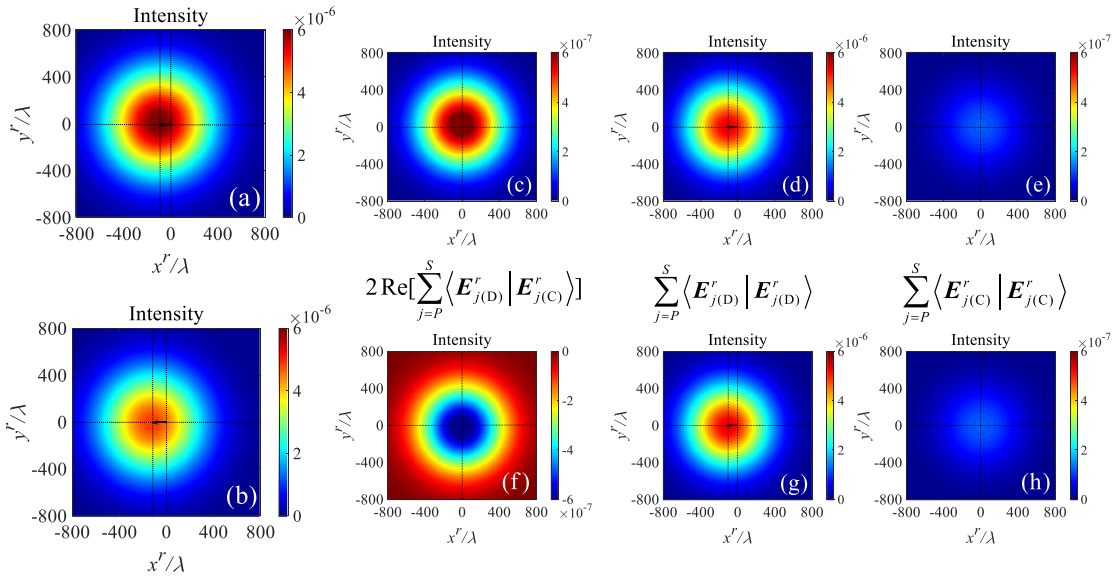

Figure 5. Reflected light field intensity distributions when an elliptically polarized beam with $\alpha = \pm 0.1^\circ$ and $\Delta\phi = 90^\circ$ strikes an air- Type II WSM film interface withθ_i =75.80°, $\alpha_t = 1.25$, $w_0 = 2000\lambda/\pi$. (a) $\alpha = -0.1^\circ$ and (e) $\alpha = +0.1^\circ$ for the total reflected light field, (b) $\alpha = -0.1^\circ$ and (f) $\alpha = +0.1^\circ$ for the abnormal interference between direct reflected light field and cross-reflected light field, (c) $\alpha = -0.1^\circ$ and (g) $\alpha = +0.1^\circ$ for the direct reflected light field, and (d) $\alpha = -0.1^\circ$ and (h) $\alpha = +0.1^\circ$ for the cross-reflected light field.

4. Conclusion

In conclusion, we have conducted a comprehensive investigation into the anomalous GH displacement observed in light reflection at the interface between air and an anisotropic medium. Our study highlights the essential role played by the spin-dependent interference effect in the reflected light field as the fundamental physical mechanism underlying the anomalous GH displacement phenomenon. By focusing on the air and type II WSM interface as a specific case, we have thoroughly analyzed the physical nature of the anomalous GH displacement resulting from the spin-dependent abnormal interference effect between the direct reflected light field and the cross-reflected light field. We have elucidated the close connection between the spin-dependent abnormal interference effect and the tilt factor of the type II WSM, providing a promising avenue for determining the degree of tilt of the Weyl nodes. This contribution holds significant importance from a fundamental standpoint, and the proposed theory can also be extended to uncover anomalous GH displacement phenomena at other anisotropic interfaces, such as those found in two-dimensional Dirac materials.

Data availability statements

The data cannot be made publicly available upon publication because no suitable repository exists for hosting data in this field of study. The data that support the findings of this study are available upon reasonable request from the authors.

Acknowledgments

This work was supported by National Natural Science Foundation of China (NSFC Grant No. 52207228), Beijing Municipal Natural Science Foundation (Grant No. 3224070), Natural Science Foundation of the Jiangsu Higher Education Institutions of China (Grant No. 20KJB416003).

Appendix A. Fresnel equation for two-dimensional WSM

We assume that a monochromatic plane wave strikes an air-WSM film interface at an arbitrary angle of incidence θ_i, as shown in figure 6. The electric field of incident polarized light can be expressed as:

$$\boldsymbol{E}^i(\boldsymbol{r},t) = E^i_P(\boldsymbol{r},t)\,\boldsymbol{e}^i_P + E^i_S(\boldsymbol{r},t)\,\boldsymbol{e}^i_S, \tag{A1}$$

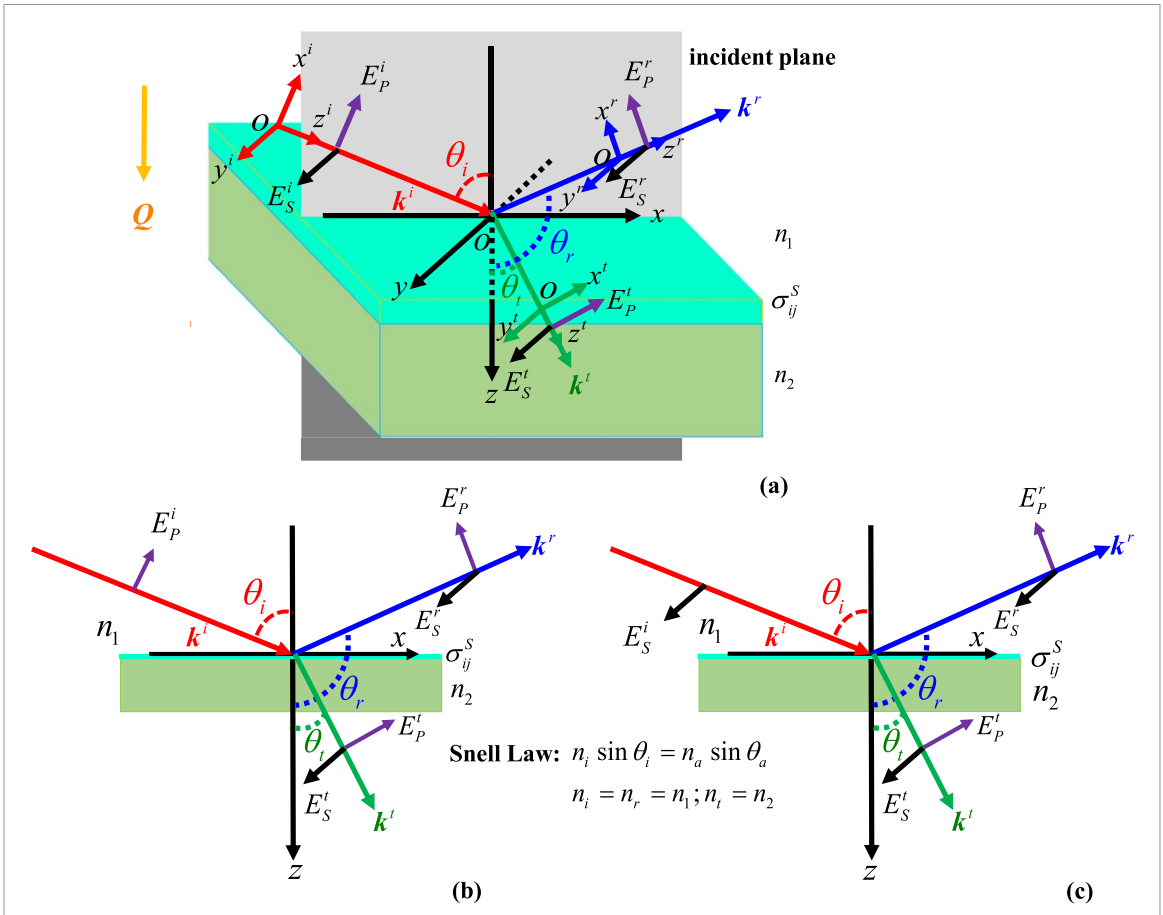

Figure 6. Schematic diagram of reflection and refraction of polarized light beams at the air-2D WSM interface. (a) Three-dimensional installation diagram; (b) $\boldsymbol{E}_P^i$ is located at the plane of incidence; (c) $\boldsymbol{E}_S^i$ is perpendicular to the plane of incidence. Here $\boldsymbol{B}$ is not drawn and $\boldsymbol{Q}$ denotes the Weyl node separation, $\sigma_{xy}, \sigma_{yx} \propto Q$, the Weyl node separation $Q = 3.2 \times 10^8\ \mathrm{m}^{-1}$, $\sigma_{xx} = \sigma_{yy} \propto \omega$, $\sigma_{ij}^S = d\sigma_{ij}$, a thin film of thickness $d = 10$ nm.

with $E_{P/S}^i(\boldsymbol{r},t) = a_{P/S}\exp[i(\boldsymbol{k}^i\cdot\boldsymbol{r}-\omega^i t)]$, $\boldsymbol{r} = x\hat{\boldsymbol{x}} + y\hat{\boldsymbol{y}} + z\hat{\boldsymbol{z}}$

where $\hat{\boldsymbol{x}}$, $\hat{\boldsymbol{y}}$ and $\hat{\boldsymbol{z}}$ represent unit vectors along the x, y, and z axes respectively and $\boldsymbol{e}_P^i$, $\boldsymbol{e}_S^i$ represent unit vectors along the x^i and y^i axes respectively.

Considering that the electromagnetic field is limited by the boundary continuity condition, the electric field expression of the incident polarized light is expanded under the $\{\hat{\boldsymbol{x}}, \hat{\boldsymbol{y}}, \hat{\boldsymbol{z}}\}$ basis to make use of the boundary continuity condition. The expression of the incident light field after expansion is as follows:

$$\boldsymbol{E}^i(\boldsymbol{r},t) = E_P^i\cos\theta_i\hat{\boldsymbol{x}} + E_S^i\hat{\boldsymbol{y}} - E_P^i\sin\theta_i\hat{\boldsymbol{z}}. \tag{A2}$$

Similarly, the electric fields of transmitted light and reflected light are respectively expressed as follows:

$$\boldsymbol{E}^t(\boldsymbol{r},t) = E_P^t\cos\theta_t\hat{\boldsymbol{x}} + E_S^t\hat{\boldsymbol{y}} - E_P^t\sin\theta_t\hat{\boldsymbol{z}}, \tag{A3}$$

$$\boldsymbol{E}^r(\boldsymbol{r},t) = E_P^r\cos\theta_r\hat{\boldsymbol{x}} + E_S^r\hat{\boldsymbol{y}} - E_P^r\sin\theta_r\hat{\boldsymbol{z}}. \tag{A4}$$

Here $E_{P,S}^a(\boldsymbol{r},t) = b_{P,S}^a\exp[i(\boldsymbol{k}^a\cdot\boldsymbol{r}-\omega^a t)]$, $a = r, t$. According to the second equation of Maxwell's equations, the relationship between the magnetic field and electric field satisfies the following:

$$\boldsymbol{B}^a(\boldsymbol{r},t) = n_a k\left(-E_S^a\boldsymbol{e}_P^a + E_P^a\boldsymbol{e}_S^a\right)/\omega^a. \tag{A5}$$

Therefore, the magnetic field expressions of incident light, transmitted light, and reflected light are respectively expressed as:

$$\boldsymbol{B}^i(\boldsymbol{r},t) = \frac{n_i k}{\omega^i}\left(-E_S^i\cos\theta_i\hat{\boldsymbol{x}} + E_P^i\hat{\boldsymbol{y}} + E_S^i\sin\theta_i\hat{\boldsymbol{z}}\right), \tag{A6}$$

$$\boldsymbol{B}^t(\boldsymbol{r},t) = \frac{n_t k}{\omega^t}\left(-E_S^t\cos\theta_t\hat{\boldsymbol{x}} + E_P^t\hat{\boldsymbol{y}} + E_S^t\sin\theta_t\hat{\boldsymbol{z}}\right), \tag{A7}$$

$$\boldsymbol{B}^r(\boldsymbol{r},t) = \frac{n_r k}{\omega^r}\left(-E_S^r\cos\theta_r\hat{\boldsymbol{x}} + E_P^r\hat{\boldsymbol{y}} + E_S^r\sin\theta_r\hat{\boldsymbol{z}}\right). \tag{A8}$$

Obviously, the electric field and magnetic field must meet the boundary conditions at the interface [58]:

$$\hat{\boldsymbol{z}}\times\left(\boldsymbol{E}^t - \boldsymbol{E}^i - \boldsymbol{E}^r\right) = 0, \tag{A9}$$

$$\hat{\boldsymbol{z}}\times\left(\boldsymbol{B}^t - \boldsymbol{B}^i - \boldsymbol{B}^r\right) = \mu\boldsymbol{J}. \tag{A10}$$

Therefore, the component expressions of equations (A9) and (A10) can be written as:

$$E_x^i + E_x^r = E_x^t, \tag{A11}$$

$$E_y^i + E_y^r = E_y^t, \tag{A12}$$

$$-B_y^t + B_y^i + B_y^r = \mu J_x, \tag{A13}$$

$$B_x^t - B_x^i - B_x^r = \mu J_y. \tag{A14}$$

Here $\boldsymbol{J}$ is the conduction current density vector. For two-dimensional anisotropic materials, the current density vector $\boldsymbol{J}$ caused by the optical field is:

$$\begin{pmatrix} J_x \\ J_y \end{pmatrix} = \begin{pmatrix} \sigma_{xx}^S & \sigma_{xy}^S \\ \sigma_{yx}^S & \sigma_{yy}^S \end{pmatrix}\begin{pmatrix} E_x^t \\ E_y^t \end{pmatrix}. \tag{A15}$$

Therefore, after substituting equation (A15) into equations (A13) and (A14), the following relation can be easily obtained:

$$-B_y^t + B_y^i + B_y^r = \mu\left(\sigma_{xx}^S E_x^t + \sigma_{xy}^S E_y^t\right), \tag{A16}$$

$$B_x^t - B_x^i - B_x^r = \mu\left(\sigma_{yx}^S E_x^t + \sigma_{yy}^S E_y^t\right). \tag{A17}$$

On the boundary surface of $z = 0$, the incident light field, transmitted light field, and reflected light field meet the boundary continuity condition at any position and at any time, which means that the variation law of these fields on the interface with space (time) must also be the same, so the frequencies of the incident, transmitted and reflected light beams must satisfy the following relation:

$$\omega^i = \omega^r = \omega^t. \tag{A18}$$

Here, equation (A18) does not consider electromagnetic waves with high intensity, so the high-order harmonic effect can be ignored. Meanwhile, the wave vectors of the incident, transmitted, and reflected light beams must satisfy the following relation:

$$\left(\boldsymbol{k}^i\cdot\boldsymbol{e}_x\right)x + \left(\boldsymbol{k}^i\cdot\boldsymbol{e}_y\right)y = \left(\boldsymbol{k}^t\cdot\boldsymbol{e}_x\right)x + \left(\boldsymbol{k}^t\cdot\boldsymbol{e}_y\right)y = \left(\boldsymbol{k}^r\cdot\boldsymbol{e}_x\right)x + \left(\boldsymbol{k}^r\cdot\boldsymbol{e}_y\right)y. \tag{A19}$$

Equation (A19) is obviously valid for any x and y on the interface, so the following relation must be satisfied:

$$n_i\sin\theta_i = n_a\sin\theta_a. \tag{A20}$$

For the convenience of the following calculation, it is obvious that equations (A11) and (A12) can be further written as:

$$E_P^i\cos\theta_i + E_P^r\cos\theta_r = E_P^t\cos\theta_t, \tag{A21}$$

$$E_S^i + E_S^r = E_S^t. \tag{A22}$$

Substituting equations (A6)–(A8) into equations (A16) and (A17), and taking into account equation (A9), the equations (A16) and (A17) can be transformed into the following form:

$$-n_t E_S^t \cos\theta_t + n_i E_S^i \cos\theta_i + n_r E_S^r \cos\theta_r = Z_0 \left[\sigma_{yx}^S E_P^t \cos\theta_t + \sigma_{yy}^S E_S^t\right], \tag{A23}$$

$$-n_t E_P^t + n_i E_P^i + n_r E_P^r = Z_0 \left[\sigma_{xx}^S E_P^t \cos\theta_t + \sigma_{xy}^S E_S^t\right] \tag{A24}$$

where $Z_0 = \mu c = \sqrt{\mu_0/\varepsilon_0}$ ($\mu_r = 1$). Substituting equations (A21) and (A22) into equation (A23), it is easy to eliminate E_P^t and E_S^t, so equation (A23) can be written as follows:

$$E_P^r = r_{PP} E_P^i + r_{PS} E_S^i. \tag{A25}$$

This evidently implies

$$r_{PP} = \frac{[(Z_0\sigma_{xx}^S \cos\theta_t + n_t)\cos\theta_i - n_i\cos\theta_t][n_r\cos\theta_r - (Z_0\sigma_{yy}^S + n_t\cos\theta_t)] + {Z_0}^2\sigma_{xy}^S\sigma_{yx}^S\cos\theta_i\cos\theta_t}{[n_r\cos\theta_r - (Z_0\sigma_{yy}^S + n_t\cos\theta_t)][n_r\cos\theta_t - (Z_0\sigma_{xx}^S\cos\theta_t + n_t)\cos\theta_r] - {Z_0}^2\sigma_{xy}^S\sigma_{yx}^S\cos\theta_r\cos\theta_t}, \tag{A26}$$

$$r_{PS} = \frac{-2Z_0\sigma_{xy}^S n_i\cos\theta_i\cos\theta_t}{[n_r\cos\theta_r - (Z_0\sigma_{yy}^S + n_t\cos\theta_t)][n_r\cos\theta_t - (Z_0\sigma_{xx}^S\cos\theta_t + n_t)\cos\theta_r] - {Z_0}^2\sigma_{xy}^S\sigma_{yx}^S\cos\theta_r\cos\theta_t}. \tag{A27}$$

Similarly, equations (A21) and (A22) can be substituted into equation (A24) to eliminate E_P^t and E_S^t, and equation (A24) can be written as

$$E_S^r = r_{SP} E_P^i + r_{SS} E_S^i. \tag{A28}$$

This implies

$$r_{SP} = \frac{2n_i Z_0\sigma_{yx}^S\cos\theta_i\cos\theta_t}{[n_r\cos\theta_t - (Z_0\sigma_{xx}^S\cos\theta_t + n_t)\cos\theta_r]\left[n_r\cos\theta_i + \left(Z_0\sigma_{yy}^S + n_t\cos\theta_t\right)\right] - {Z_0}^2\sigma_{yx}^S\sigma_{xy}^S\cos\theta_t\cos\theta_i}, \tag{A29}$$

$$r_{SS} = -\frac{{Z_0}^2\sigma_{yx}^S\sigma_{xy}^S\cos\theta_t\cos\theta_r + \left[n_r\cos\theta_t - \left(Z_0\sigma_{xx}^S\cos\theta_t + n_t\right)\cos\theta_r\right]\left[\left(Z_0\sigma_{yy}^S + n_t\cos\theta_t\right) - n_i\cos\theta_i\right]}{[n_r\cos\theta_t - (Z_0\sigma_{xx}^S\cos\theta_t + n_t)\cos\theta_r]\left[n_r\cos\theta^i + \left(Z_0\sigma_{yy}^S + n_t\cos\theta_t\right)\right] - {Z_0}^2\sigma_{yx}^S\sigma_{xy}^S\cos\theta_t\cos\theta_i}. \tag{A30}$$

By using the relations $n_r = n_i = n_1$, $n_t = n_2$, $\sigma_{xy}^S = -\sigma_{yx}^S$, and $\cos\theta_r = -\cos\theta_i$, the formulas (10)–(12) of Fresnel equations in the reflection case are obtained.

Appendix B. The Type II WSM transverse optical conductivity for He–Ne laser wavelength

The degree of tilt of the Weyl nodes is characterized by α_t, with $|\alpha_t| < 1$ being a type-I Weyl node, and $|\alpha_t| > 1$ being a type-II Weyl node [59]. For the Type-II WSM with $|\alpha_t| > 1$, the real and imaginary parts of the transverse photoconductivity σ_{xx} satisfy the following relation:

$$\mathrm{Re}\left[\sigma_{xx}(\omega)\right]\begin{cases} = 0 & I \quad \omega < \omega_l \\ = \sigma_\omega\left(\frac{1}{2} - \eta_1\right) & II \quad \omega_l < \omega < \omega'_\mu \\ = \sigma_\omega\eta_2 & III \quad \omega > \omega'_\mu \end{cases}, \tag{B1}$$

$$\mathrm{Im}\left[\sigma_{xx}(\omega)\right] = -\frac{\sigma_\omega}{4\pi}\left\{\tau(\alpha_t)\ln\left[\frac{\left|{\omega'_\mu}^2 - \omega^2\right|}{\left|\omega_l^2 - \omega^2\right|}\right] + \frac{8}{|\alpha_t|^3}\left(\frac{\mu}{\hbar\omega}\right)^2 - \left(\frac{\mu}{\hbar\omega}\right)^3 \Pi(\omega, \alpha_t, \mu)\ln\left[\frac{\left|\omega'_\mu - \omega\right|(\omega_l + \omega)}{\left|\omega_l - \omega\right|(\omega'_\mu + \omega)}\right]\right.$$
$$\left. + \frac{6}{|\alpha_t|^3}\left(\frac{\mu}{\hbar\omega}\right)^2\ln\left[\frac{\left|{\omega'_\mu}^2 - \omega^2\right|\omega_l^2}{\left|\omega_l^2 - \omega^2\right|{\omega'_\mu}^2}\right] + \left(\frac{3}{|\alpha_t|} + \frac{1}{|\alpha_t|^3}\right)\ln\left[\frac{\left|\omega_c^2 - \omega^2\right|}{\left|{\omega'_\mu}^2 - \omega^2\right|}\right] + \frac{12}{|\alpha_t|^3}\left(\frac{\mu}{\hbar\omega}\right)^2\ln\left[\frac{\left|\omega_c^2 - \omega^2\right|{\omega'_\mu}^2}{\left|{\omega'_\mu}^2 - \omega^2\right|\omega_c^2}\right]\right\}, \tag{B2}$$

with

$$\sigma_\omega = e^2\omega/(6h v_F),$$

$$\eta_1 = \frac{3}{8|\alpha_t|}\left(\frac{2\mu}{\hbar\omega}-1\right)\left[1+\frac{1}{3|\alpha_t|^2}\left(\frac{2\mu}{\hbar\omega}-1\right)^2\right], \eta_2 = \frac{3}{4|\alpha_t|}\left[1+\frac{1}{3|\alpha_t|^2}+\left(\frac{2\mu}{|\alpha_t|\hbar\omega}\right)^2\right],$$
$$\omega_l = 2\mu/[\hbar(1+|\alpha_t|)], \omega_\mu = 2\mu/[\hbar(|\alpha_t|-1)],$$
$$\tau(\alpha_t) = \frac{1}{2}\left(4+\frac{3}{|\alpha_t|}+\frac{1}{|\alpha_t|^3}\right)$$
$$\Pi(\omega,\alpha_t,\mu) = \frac{4}{|\alpha_t|^3}+3\left(\frac{\mu}{\hbar\omega}\right)^2\left(\frac{1}{|\alpha_t|}+\frac{1}{|\alpha_t|^3}\right),$$
$$\eta_1 = \frac{3}{8|\alpha_t|}\left(\frac{2\mu}{\hbar\omega}-1\right)\left[1+\frac{1}{3|\alpha_t|^2}\left(\frac{2\mu}{\hbar\omega}-1\right)^2\right], \eta_2 = \frac{3}{4|\alpha_t|}\left[1+\frac{1}{3|\alpha_t|^2}+\left(\frac{2\mu}{|\alpha_t|\hbar\omega}\right)^2\right],$$

where $\omega_c = v_F k_c$ is the ultraviolet cutoff frequency ($v_F$is the Fermi velocity, $k_c = \pi/a$ is the cutoff along the kz direction, the lattice spacing $a = 10$ nm), and μ is the chemical potential. For equation (B1), it is worth stating that the region of $\omega < \omega_l$ (region I) is completely Pauli blocked for vertical transitions, while the $\omega_l < \omega < \omega'_\mu$ (region II), is partially Pauli blocked for vertical transitions, and $\omega > \omega'$ (region III), the full phase space is available for vertical transitions.

In addition, the real part of transverse photoconductivity σ_{xy} can be expressed as:

$$\mathrm{Re}\left[\sigma_{xy}(\omega)\right] = \mathrm{Re}\left(\sigma_{xy}^{dc}\right) + \mathrm{Re}\left(\sigma_{xy}^{ac}\right). \tag{B3}$$

Here, the dc and ac components for $\mathrm{Re}[\sigma_{xy}(\omega)]$ can be written respectively

$$\mathrm{Re}\left(\sigma_{xy}^{dc}\right) = \frac{\sigma_Q}{|\alpha_t|} + \frac{\mathrm{sgn}(\alpha_t)\sigma_\mu}{{\alpha_t}^2}\ln\left[\frac{\mu^2}{\hbar^2\omega_c^2{\alpha_t}^2({\alpha_t}^2-1)}\right],$$

$$\mathrm{Re}\left(\sigma_{xy}^{ac}\right) = \mathrm{sgn}(\alpha_t)\sigma_\mu\left\{-\frac{1}{2{\alpha_t}^2}\ln\left[\frac{\left(\omega_c^2-\omega^2\right)^2}{\left|\omega_l^2-\omega^2\right|\left|{\omega'_\mu}^2-\omega^2\right|}\frac{\omega_l^2{\omega'_\mu}^2}{\omega_c^4}\right] + \left(\frac{\mu}{2\hbar\omega{\alpha_t}^2}+\frac{\hbar\omega}{8\mu}\frac{1-{\alpha_t}^2}{{\alpha_t}^2}\right)\right.$$
$$\left.\times\ln\left[\frac{|\omega'_\mu-\omega|(\omega_l+\omega)}{(\omega'_\mu+\omega)(\omega_l-\omega)}\right]-\frac{2}{{\alpha_t}^2}\right\}$$

where $\sigma_\mu = \frac{e^2\mu}{\hbar^2 v_F}$ and $\sigma_\mu = \frac{e^2 Q}{\pi\hbar}$.

Finally, the expression for the imaginary part of the transverse photoconductivity σ_{xy} can be written as follows:

$$\mathrm{Im}\left[\sigma_{xy}(\omega)\right]\begin{cases} = 0 & I \quad \omega < \omega_l \\ = 3\sigma_\omega\eta_3 & II \quad \omega_l < \omega < {\omega'}_\mu \\ = -3\mu\sigma_\omega/\left(\hbar\omega\alpha_t^2\right) & III \quad \omega > {\omega'}_\mu \end{cases} \tag{B4}$$

In the simulation, we have chosen $\lambda = 632.8$ nm, $\mu = 0.125$ eV, and $1.25 < \alpha_t < 3.25$, then the relation $\omega > \omega'_\mu$ is satisfied. Therefore, transverse photoconductivity $\mathrm{Re}[\sigma_{xx}(\omega)]$ and $\mathrm{Im}[\sigma_{xy}(\omega)]$ in this work are determined by expression III in equations (B1) and (B4) respectively.

ORCID iDs

Ze Chen https://orcid.org/0000-0003-2013-1887
Yang Meng https://orcid.org/0000-0001-6559-5242

References

[1] Newton I 1992 *Opticks* Reprint edn (Dover Press)
[2] Goos F and Hänchen H 1947 *Ann. Phys.* **436** 333
[3] Artmann K 1948 *Ann. Phys.* **437** 87
[4] Bliokh K Y and Aiello A 2013 *J. Opt.* **15** 014001
[5] Wang L, Chen H and Zhu S 2005 *Opt. Lett.* **30** 2936
[6] Chen X, Chun-Fang L and Ban Y 2008 *Phys. Rev.* A **77** 073307
[7] Li C F and Wang Q 2004 *Phys. Rev.* E **69** 055601
[8] Chen X and Li C-F 2004 *Phys. Rev.* E **69** 066617
[9] Liu X, Cao Z, Zhu P, Shen Q and Liu X 2006 *Phys. Rev.* E **73** 056617

[10] Chen L, Cao Z, Ou F, Li H, Shen Q and Qiao H 2007 *Opt. Lett.* **32** 1432
[11] Wu F *et al* 2021 *Phys. Rev.* A **104** 023518
[12] Foster D H, Cook A K and Nöckel J U 2007 *Opt. Lett.* **32** 1764
[13] Unterhinninghofen J, Wiersig J and Hentschel M 2008 *Phys. Rev.* E **78** 016201
[14] Yu T, Li H, Cao Z, Wang Y, Shen Q and He Y 2008 *Opt. Lett.* **33** 1001
[15] Wang X, Cheng Y, Sun J, Li H, Wang Y, Ran M and Cao Z 2013 *Opt. Express* **21** 13380
[16] Li C F 2003 *Phys. Rev. Lett.* **91** 133903
[17] Li C F 2007 *Phys. Rev.* A **76** 013811
[18] Merano M, Aiello A, van Exter M P and Woerdman J P 2009 *Nat. Photon.* **3** 337
[19] Wan Y, Zheng Z and Zhu J 2009 *Opt. Express* **17** 21313
[20] Aiello A and Woerdman J P 2011 *Opt. Lett.* **36** 3151
[21] Löffler W, Aiello A and Woerdman J P 2012 *Phys. Rev. Lett.* **109** 213901
[22] Aiello A 2012 *New J. Phys.* **14** 013058
[23] Xiao Z, Luo H and Wen S 2012 *Phys. Rev.* A **85** 053822
[24] Wang L G, Zhu S Y and Zubairy M S 2013 *Phys. Rev. Lett.* **111** 223901
[25] Araújo M P, De Leo S and Maia G 2017 *Phys. Rev.* A **95** 053836
[26] Lin H, Zhu W, Yu J, Jiang M, Zhuo L, Qiu W, Dong J, Zhong Y and Chen Z 2018 *Opt. Express* **26** 5810
[27] Zhu W, Guan H, Lu H, Tang J, Li Z, Yu J and Chen Z 2018 *Opt. Express* **26** 17378
[28] Gao M, Wang G, Yang X, Liu H and Deng D 2020 *Opt. Express* **28** 28916
[29] Jayaswal G, Mistura G and Merano M 2013 *Opt. Lett.* **38** 1232
[30] Zeng X, Al-Amri M and Zubairy M S 2017 *Opt. Express* **25** 23579
[31] Wong Y, Miao Y, Skarda J and Solgaard O 2018 *Opt. Lett.* **43** 2803
[32] Zhen W and Deng D 2020 *Opt. Express* **28** 24104
[33] Zhen W and Deng D 2020 *Opt. Commun.* **474** 126067
[34] Zhen W and Deng D 2020 *Appl. Phys.* B **126** 35
[35] Wu J, Wu F, Lv K, Guo Z, Jiang H, Sun Y, Li Y and Chen H 2020 *Phys. Rev.* A **101** 053838
[36] Zhen W and Deng D 2020 *J. Phys. D: Appl. Phys.* **53** 255104
[37] Wang H and Zhang X 2011 *Phys. Rev.* A **83** 053820
[38] Xu G, Zang T, Mao H and Pan T 2011 *Phys. Rev.* A **83** 053828
[39] Kort-Kamp W J M, Sinitsyn N A and Dalvit D A R 2016 *Phys. Rev.* B **93** 081410
[40] Wu W, Chen S, Mi C, Zhang W, Luo H and Wen S 2017 *Phys. Rev.* A **96** 043814
[41] Chen Z, Zhang H, Zhang X, Li H , Zhang W and Xi L 2020 *Opt. Express* **28** 8308
[42] Ye G, Zhang W, Wu W, Chen S, Shu W, Luo H and Wen S 2019 *Phys. Rev.* A **99** 023807
[43] Liu S, Song Y, Wan T, Ke Y and Luo Z 2022 *Chin. Phys.* B **31** 074101
[44] Yue Q, Zhou X and Deng D 2023 *New J. Phys.* **25** 018001
[45] Cui N, Zhang X, Zheng Z, Xu H, Zhang W, Tang X, Xi L, Fang Y and Li L 2018 *Opt. Express* **26** 21170
[46] Bliokh K Y and Bliokh Y P 2007 *Phys. Rev.* E **75** 066609
[47] Aiello A and Woerdman J P 2009 (arXiv:0903.3730)
[48] Deng K *et al* 2016 *Nat. Phys.* **12** 1105
[49] Wang Z, Gresch D, Soluyanov A A, Xie W, Kushwaha S, Dai X, Troyer M, Cava R J and Bernevig B A 2016 *Phys. Rev. Lett.* **117** 056805
[50] Sonowal K, Singh A and Agarwal A 2019 *Phys. Rev.* B **100** 085436
[51] Chen S, Mi C, Wu W, Zhang W, Shu W, Luo H and Wen S 2018 *New J. Phys.* **20** 103050
[52] Bansil A, Lin H and Das T 2016 *Rev. Mod. Phys.* **88** 021004
[53] Jia G, Huang Z, Ma Q and Li G 2019 *Nanophotonics* **9** 715
[54] Jia G, Zhang R, Huang Z, Ma Q, Wang H and Asgari R 2021 *New J. Phys.* **23** 073010
[55] Liu S, Yang C, Song Y, Tang P, Ke Y and Luo Z 2021 *J. Appl. Phys.* **54** 285108
[56] Wu J, Jiang L, Zeng R, Liang J, Dai X and Xiang Y 2022 *Phys. Rev.* A **105** 023508
[57] Da H, Song Q and Ye H 2022 *Opt. Lett.* **47** 4359
[58] Born M and Wolf E 2003 *Principles of Optics* 7th edn (Cambridge University Press)
[59] Sonowal K, Singh A and Agarwal A 2019 *Phys. Rev.* B **100** 085436